

ARTICLES

Enhanced spin polarization of conduction electrons in Ni explained by comparison with Cu

K. N. Altmann and D. Y. Petrovykh

Department of Physics, University of Wisconsin at Madison, 1150 University Avenue, Madison, Wisconsin 53706-1390

G. J. Mankey

MINT Center, University of Alabama, Box 870209, Tuscaloosa, Alabama 35487-0209

N. Shannon

Department of Physics, University of Wisconsin at Madison, 1150 University Avenue, Madison, Wisconsin 53706-1390

N. Gilman, M. Hochstrasser, and R. F. Willis

Department of Physics, Penn State University, University Park, Pennsylvania 16802-6300

F. J. Himpsel

Department of Physics, University of Wisconsin at Madison, 1150 University Avenue, Madison, Wisconsin 53706-1390

(Received 6 January 2000)

The spin-split Fermi-level crossings of the conduction band in Ni are mapped out by high-resolution photoemission and compared to the equivalent crossing in Cu. The area of the quasiparticle peak decreases rapidly below E_F in Ni, but not in Cu. Majority spins have larger spectral weight at E_F than minority spins, thereby enhancing the spin polarization beyond that expected from the density-of-states. A large part of the effect can be traced to a rapid variation of the matrix element with \mathbf{k} at the point where the s,p band begins to hybridize with the d_z^2 state. However, it is quite possible that the intensity drop in Ni is reinforced by a transfer of spectral weight from single-particle to many-electron excitations. The results suggest that the matrix element should be considered for explaining the enhanced spin polarization observed for Ni in spin-polarized tunneling.

I. SPIN-POLARIZED CURRENTS IN MAGNETOELECTRONICS

The rapidly growing field of magnetoelectronics¹⁻³ is largely based on the manipulation of spin currents that are carried by electrons at the Fermi level E_F . Examples are the application of giant magnetoresistance in reading heads for hard disks and the use of spin-polarized tunneling^{4,5} and junction magnetoresistance for a magnetic random access memory. Spin-polarized tunneling is also being explored for high-resolution magnetic imaging by scanning tunneling microscopy (STM).⁶⁻⁸ The magnitude of the magnetoresistance increases with the spin polarization of the currents, likewise the magnetic contrast in STM. A variety of efforts are directed towards designing new magnetic materials with higher spin polarization, such as half-metallic compounds and nanostructures. For making systematic progress one first has to identify the electronic states that are responsible for the spin currents, then determine the fundamental parameters relevant for spin polarization, and eventually apply this knowledge to the design of new magnetic materials.

The character of the spin carriers in ferromagnets has been debated for some time.⁹⁻¹⁷ The initial puzzle has been whether s,p , or d electrons dominate transport properties.⁹ The s,p -states have high group velocity, but low-density-of-

states and weak magnetism. The d states carry the magnetic moment and have high-density-of-states, but their group velocity is low. This dilemma can be resolved by looking at a realistic band structure where a free-electronlike s,p band hybridizes with the magnetic d levels close to the Fermi level.^{9,15} That allows the s,p band to acquire a significant magnetic splitting.¹⁴⁻¹⁶

The origin of the spin polarization is still under intense investigation.¹⁰⁻¹⁷ Various mechanisms have been proposed, such as a spin dependence of the density-of-states, spin-dependent electron scattering in the bulk and at interfaces, and a spin-dependent matrix element. A direct determination of the spin polarization from magnetotransport properties is difficult. An extensive set of values has been reported for spin-polarized tunneling into superconductors^{4,5} and Andreev reflection at point contacts to superconductors.^{18,19} The traditional explanation of such data has been the imbalance in the density-of-states at E_F for a magnetically-split free-electron band.⁴ It has been fairly successful for explaining the spin polarization of Fe, but has failed for Ni where the observed spin polarization of 23%–46% far exceeds the 6% spin polarization expected from the density-of-states.^{4,5,18,19} A variety of more sophisticated approaches have been proposed for explaining spin-polarized tunneling.^{10-13,17} It is highly desirable to achieve high spin polarization in tunnel-

ing from Ni alloys, such as permalloy ($\text{Ni}_{0.8}\text{Fe}_{0.2}$), since permalloy is the most common material in magnetoelectronics.

It is difficult to pinpoint the parameters relevant for achieving high spin polarization from transport data alone. Such measurements integrate in \mathbf{k} space over the Fermi surface and involve additional parameters, such as scattering lengths. Angle-resolved photoemission is able to focus onto specific \mathbf{k} points²⁰ and to separate out scattering lengths.¹⁴ Traditionally, this technique has lacked sufficient energy resolution for discerning the electronic states that are relevant for transport phenomena, that is those within a few thermal energies kT of E_F . In our paper the energy resolution is 9 meV for electrons plus photons, compared to $kT = 25$ meV at room temperature. Tunable synchrotron radiation allows us to map out the \mathbf{k} component perpendicular to the surface independent of the parallel components. As non-magnetic reference material we use Cu. It has the same crystal structure as the adjacent Ni and a similar band topology. The main difference is an energy shift of the d bands, which lie 2 eV lower in Cu than in Ni.

Our key observations are two intensity anomalies in the spin-split Ni conduction band: Below E_F the band loses intensity very rapidly in Ni but not in Cu. Furthermore, majority spins have larger photoemission intensity at E_F than minority spins. That creates an extra spin polarization beyond the higher density-of-states for majority spins (which enters when integrating \mathbf{k} over the Fermi surface). Several possible explanations are explored, such as increased electron scattering below E_F , a photoemission matrix element that varies rapidly with E and \mathbf{k} , and a transfer of spectral weight from single-electron excitations to many-electron excitations. Judging from our comparison with Cu and from simple matrix element calculations we assign the anomalies in Ni in large part to a rapid decrease of the matrix element at the point where the s,p band becomes more d -like. Our finding suggests that a similar role can be expected from the matrix element in other phenomena, such as in spin-polarized tunneling.

II. MANY-BODY STATES, SPECTRAL FUNCTION, AND MATRIX ELEMENT

For encompassing the possibility of many-body interactions and electron scattering it is useful to start out with a very general characterization of electronic states in solids. That can be achieved by a spectral function $A(\omega, \mathbf{k})$ which describes the spectral weight as a function of energy $E = \hbar\omega$ and momentum $\mathbf{p} = \hbar\mathbf{k}$. In a band-structure model, where only single-electron excitations are possible, $A(\omega, \mathbf{k})$ consists of sharp δ -function peaks. The spectral function is far more general than this, however, and can describe all the many-electron effects measurable in a photoemission experiment. This generality is particularly useful for describing correlated electrons in the partially-filled $3d$ -shells of ferromagnets. Ni exhibits a broad satellite several eV below the single-hole states,^{21–28} which may be viewed as a pair of correlated d holes. The consequences of the two-hole satellite for the single-particle excitations in Ni are a reduction of the bandwidth by 40% and a decrease of the magnetic splitting by a factor of 2–3.^{24–27} These discrepancies have been associated with spectral weight shifting from the single-hole

d bands down to the two-hole satellite while preserving the center-of-gravity of the energy spectrum. A trading of spectral weight between single- and multielectron excitations has been observed in adsorbates²⁹ and oxides,³⁰ too.

Such a many-body effect will be considered as one of two plausible explanations for the drop of the photoemission intensity below E_F in Ni. The line of thought is the following: The conduction band in Ni is s,p -like above E_F but acquires more d character below E_F as it starts hybridizing with the d bands. The increasing d character makes it prone to many-electron effects, such as a transfer of spectral weight to the two-hole satellite. Even the smaller intensity of the minority-spin peak at E_F would find a natural explanation in such a scenario, because the minority-spin d bands lie higher in energy and hybridize more with the minority-spin conduction band at E_F . For assessing this hypothesis, we use Cu as reference material where many-electron effects are weak. For example, the intensity of the two-hole satellite is 21% of the one-hole states in Ni, but only 2.5% in Cu.²³

The spectral function $A(\omega, \mathbf{k})$ is related to the angle-resolved photoemission intensity $I(\omega, \mathbf{k})$ by a matrix element $M(\omega, \mathbf{k})$, that is specific to the photoemission process:³¹

$$I(\omega, \mathbf{k}) = A(\omega, \mathbf{k}) |M(\omega, \mathbf{k})|^2 f(\omega). \quad (1)$$

The Fermi-Dirac function $f(\omega)$ gives the occupancy. The spectral function itself has the form

$$A(\omega, \mathbf{k}) = -\pi^{-1} \text{Im} [1/[\omega - E_0(\mathbf{k}) - \Sigma(\omega, \mathbf{k})]], \quad (2)$$

containing the complex self-energy $\Sigma(\omega, \mathbf{k})$ and the electron band dispersion $E_0(\mathbf{k})$. A fundamental sum rule for the spectral function implies a trade off between single-electron and many-electron excitations:

$$\int A(\omega, \mathbf{k}) d\omega = 1. \quad (3)$$

The Fermi-Dirac function is absent, thus requiring an extrapolation of photoemission data above the Fermi level, or the inclusion of inverse photoemission data. One remaining piece in Eq. (1) to be determined, is the matrix element $M(\mathbf{k})$ for single-hole excitations from the Σ_1 band:

$$M(\mathbf{k}) = \langle \Psi_{\text{final}}(\mathbf{k}) | \mathbf{A} \cdot \mathbf{p} | \Psi_{\text{initial}}(\mathbf{k}) \rangle, \quad (4)$$

where \mathbf{A} is the vector potential of the photon and \mathbf{p} the momentum operator. We have performed an estimate of $M(\mathbf{k})$ by using a combined interpolation scheme that takes the correct bandwidth and splitting of the Ni d bands into account.³²

III. THE PHOTOEMISSION EXPERIMENT

In photoemission, the parallel component \mathbf{k}^{\parallel} is conserved and can be determined directly from the kinetic energy E_{kin} and the polar angle ϑ of the photoelectrons. The perpendicular component k^{\perp} varies with the photon energy $h\nu$ and can be estimated using a free-electron upper band with an inner potential.^{20,33} In order to obtain a clear-cut spectral function we designed the experimental geometry such that it isolates a single band crossing the Fermi level with a high photoemission cross section. This is achieved by selecting the Σ_1 conduction band along the [110] direction in \mathbf{k} space. It crosses

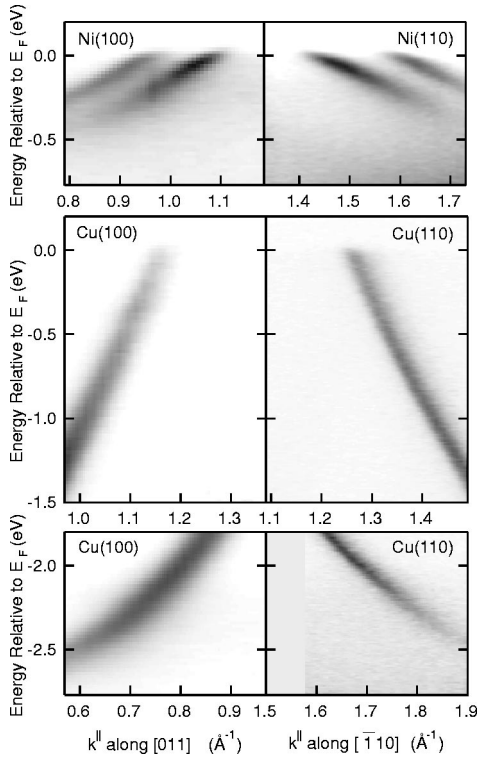


FIG. 1. E versus k^{\parallel} band dispersions of Ni and Cu near the Fermi level E_F , obtained by parallel detection of E and ∂ . In Ni, the spectral weight drops rapidly below E_F (top), in Cu it increases (center). Cu behaves similar to Ni when looking at 2 eV lower energies, where the d hybridization is comparable (bottom). The Σ_1 conduction band is mapped from two surfaces at different photon energies in opposite directions (left and right). The gray scale represents high-photoemission intensity as dark.

E_F about halfway between Γ and X and stays as far from the d bands as possible.³³ Dipole selection rules provide additional selectivity: The choice of p -polarized light with the electric field vector in the photoemission plane enhances the Σ_1 band due to its even mirror symmetry and eliminates d bands with odd symmetry. As a result, the photoemission data in Fig. 1 clearly show a single conduction band for Cu and a spin-split version of that band for Ni.

As consistency check we map the same Fermi-level crossing from two different surfaces, the (100) and the (110). For the (100) surface we reach the desired location³³ with a photon energy $h\nu=44$ eV for Ni ($h\nu=50$ eV for Cu), combined with a polar angle of about 20° along the $[011]$ azimuth. The (110) surface probes the same \mathbf{k} point with a photon energy $h\nu=27$ eV and a polar angle of about 35° along $[\bar{1}10]$. For the (100) surface one starts at Γ for $k^{\parallel}=0$ and reaches X at $k^{\parallel}=\sqrt{2}2\pi/a=2.52\text{ \AA}^{-1}$ in Ni (2.46 \AA^{-1} in Cu). For the (110) surface the bands are mapped in reverse, starting at X for $k^{\parallel}=0$ and reaching Γ at $k^{\parallel}=\sqrt{2}2\pi/a$. This inverted \mathbf{k} scale shows up in Fig. 1 as an approximate mirror symmetry of the (100) results (left) and the (110) results (right).

Comparing the intensities near E_F one finds opposite behavior for Ni and Cu (Fig. 1 top versus center). The Ni bands fade very quickly below E_F , whereas the Cu band remains strong and even increases its intensity slightly. Losing oscillator strength so rapidly in Ni presents a puzzle: Where did the spectral weight go that ought to be there according to the

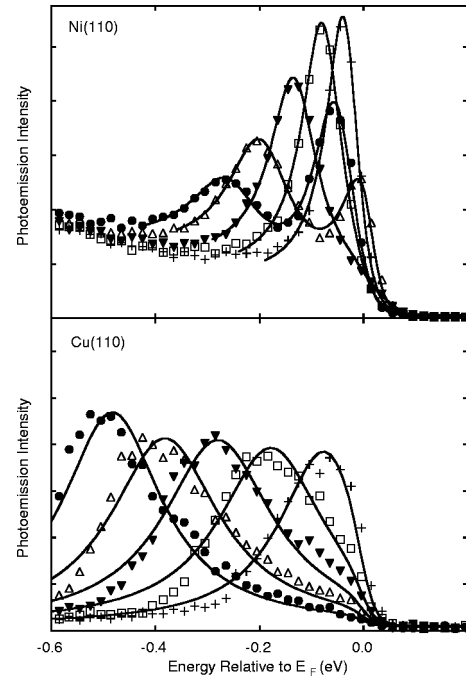


FIG. 2. Photoelectron spectra of Ni(110) and Cu(110) versus k^{\parallel} (symbols, corresponding to vertical cuts in Fig. 1). The lines represent a fit by a Lorentzian spectral function [Eq. (5)].

sum rule in Eq. (3)? Simple technical explanations fail. The \mathbf{k} acceptance of the analyzer would give equal trends for the intensity in Ni and Cu, contrary to the drop in Ni and increase in Cu. One could argue that the linewidth increases rapidly below E_F in Ni, thereby reducing the peak height. This lifetime broadening is due to the rapidly-increasing phase space for creating electron-hole pairs in the $3d$ bands of Ni. This hypothesis is discarded by fitting individual energy spectra at various \mathbf{k} with Lorentzians in Fig. 2 and plotting the resulting peak areas in Fig. 3. The drop off in Ni remains and contrasts with a slight increase in Cu.

The Lorentzian fit is equivalent to a simplified spectral function

$$A_0(\omega, \mathbf{k}) = \pi^{-1} \Gamma(\mathbf{k}) / \{[\omega - E(\mathbf{k})]^2 + \Gamma(\mathbf{k})^2\}, \quad (5)$$

where the self-energy Σ is taken as functions of \mathbf{k} only, not of ω .³⁴ The real part of $\Sigma(\mathbf{k})$ is incorporated into the empirical band dispersion $E(\mathbf{k})=E_0(\mathbf{k})+\text{Re}[\Sigma(\mathbf{k})]$. The imaginary part $\Gamma(\mathbf{k})=-\text{Im}[\Sigma(\mathbf{k})]$ describes a Lorentzian lifetime broadening. A small secondary electron background is added for fitting the data, which describes “extrinsic” energy losses of the photoelectrons on their way out. It consists of an integral over the Lorentzian line, which is equivalent to a steplike loss function.

In addition to the intensity drop below E_F there is a second anomaly in Ni. The area of the minority peak is smaller than that of the majority peak. This can be seen best from the \mathbf{k} distribution of the photoemission intensity at E_F in Fig. 4. The area ratio is $I_{\uparrow}/I_{\downarrow}=1.8$ for Ni(100) and $I_{\uparrow}/I_{\downarrow}=1.2$ for Ni(110). According to a single-electron band model one would expect very similar spectral weights for the two spin components, since they are so close together in \mathbf{k} space. In fact, previous photoelectron spectra of the spin-split bands in Ni have usually been fitted with equal intensities for the two

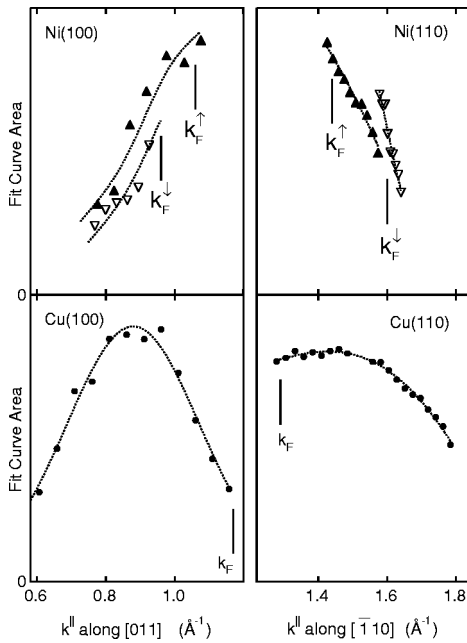


FIG. 3. Spectral weight in Ni and Cu versus k^{\parallel} , obtained from the area of the Lorentzian fit in Fig. 2 [Eq. (5)]. Note the opposite behavior of Ni and Cu near k_F .

spins. We are able to unambiguously resolve the two components by measuring a \mathbf{k} distribution at E_F , where the lifetime broadening is minimal. This spin asymmetry and the intensity drop in Ni are not sensitive to adsorbates (such as residual gas, a Cu overlayer), establishing them as pure bulk phenomena.

IV. POSSIBLE EXPLANATIONS FOR THE ANOMALIES IN Ni

Within the framework established in Eqs. (1)–(4) there are two places where one can search for an explanation of the anomalous behavior of Ni relative to Cu. These are the matrix element $|M(\omega, \mathbf{k})|^2$ and the spectral function $A(\omega, \mathbf{k})$.

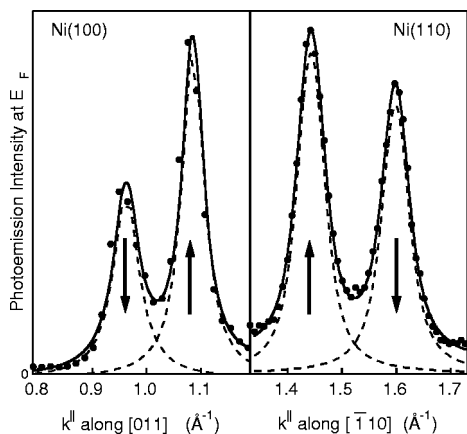


FIG. 4. Momentum distributions at E_F for Ni(110) and Ni(100), corresponding to horizontal cuts in Fig. 1 (top). The two spin components of the Σ_1 conduction band are resolved (arrows). The larger area of the majority-spin peak indicates an extra spin-polarization, beyond that expected from the larger size of the majority-spin Fermi surface.

As long as one wants to stay within the one-electron picture, the matrix element for excitation of single holes is the natural starting point. We have applied a combined interpolation scheme to the empirical band structures of Ni and Cu for obtaining estimates of $|M(\mathbf{k})|^2$.³² The result describes the (100) data qualitatively, including the opposite intensity trends for Ni and Cu. However, quantitative comparisons are fairly sensitive to the exact location of k_F , and the (110) data are not reproduced well. Clearly, more sophisticated calculations of the photoemission intensity are called for, such as the one-step model with evanescent surface wave functions. In the absence of quantitative calculations we use experimental results for explaining how the matrix element modifies the intensities in Ni and Cu. The key will be a rapid change in the hybridization between the s, p band and the $3d$ bands with energy.

While the Σ_1 conduction band corresponds to the s, p_z states in Cu, its symmetry allows for significant d_z^2 character in Ni. The Ni $3d$ states lie close to E_F and strongly hybridize with the conduction band, whereas the Cu $3d$ states lie 2 eV lower. For finding a d hybridization in Cu comparable to that of Ni one has to look 2 eV lower in energy, as shown in the bottom panels in Fig. 1. The group velocity, i.e., the slope of the Cu conduction band is greatly reduced at this point and has become comparable to that of the Ni. This is the result of an avoided crossing with the d_z^2 level.³³ Likewise, the intensity of the Cu band decreases strongly at these lower energies, similar to Ni below E_F . The same situation is surveyed in \mathbf{k} space in Fig. 3. Ni and Cu behave similar if one shifts the Ni data to the point of comparable d hybridization in Cu, i.e., a shift to the left for (100) and to the right for (110). A calculation of the matrix element³² for (100) reproduces this effect qualitatively. From such similarities between the Ni bands at E_F and the Cu bands at 2 eV below E_F , we conclude that the intensity changes in Ni are qualitatively consistent with a change in the matrix element due to increasing d hybridization.

The imbalance between the two spin components can be explained in similar fashion. The minority spin conduction band is more d -like at E_F than its majority partner since it hybridizes with the higher-lying minority d_z^2 level. Therefore, its matrix element has decreased more than that of the majority band. The consequence is an enhanced spin polarization at E_F , which has implications for spin transport phenomena, such as spin-polarized tunneling^{4,5} and Andreev reflection at ferromagnetic point contacts.^{18,19} As mentioned above, the traditional density-of-states model fails to explain the high-spin polarization observed in these experiments for Ni. The larger size of the majority spin Fermi surface in Ni would give only 6% spin polarization, compared to the observed 23%–46%. The extra spin polarization that we find at E_F enhances the density-of-states effect and brings theory closer to experiment. For a quantitative comparison it will be necessary to map this polarization across the whole Fermi surface and to replace the photoemission matrix element by the tunneling matrix element.

Despite the qualitative success of the single-particle picture one ought to consider the many-body effects in Ni. Excitations of two d holes are well documented in this material.^{21–24} Can they produce an effect similar to the decrease of the matrix element with increasing d hybridization?

There is a scenario where two-hole excitations steal spectral weight from the single-hole band, taking advantage of the sum rule in Eq. (3). It is not unreasonable to assume that the probability for exciting a pair of d holes increases with the d character of the band. Therefore, the same arguments as in the previous two paragraphs can be used, where increasing d character of the band gives rise to a decreasing matrix element. It appears that only quantitative calculations of the matrix element can settle this issue. However, there are some interesting clues pointing towards a contribution of two-hole effects. The intensity drop in Ni is more abrupt than that in Cu at the point of comparable d hybridization. This is particularly pronounced for the (110) surfaces (Fig. 3, right). One might expect a sharper drop off for a two-hole process that scales like the square of the d hybridization. An additional clue comes from the decreasing strength of two-hole excitations across the Periodic Table from Ni to Co and Fe.²³ If many-body effects played a role in the spin polarization at E_F , their influence would gradually fade from Ni to Co and Fe. Such a trend would nicely fit the results from spin-polarized tunneling, where the (one-electron) density-of-states model works best for Fe and worst for Ni.⁴

V. SUMMARY

In summary, we find a rapid loss of spectral weight in the conduction band of Ni below the Fermi level E_F , which is opposite to the behavior of the analogous band in Cu. Pos-

sible mechanisms are considered, such as an increasing lifetime broadening, the single-hole matrix element, and many-hole excitations stealing spectral weight from single-hole excitations below E_F . The comparison with Cu and a simple estimate of the matrix element indicate that the single-hole matrix element is able to give a qualitative explanation. An additional transfer of spectral weight to two-hole states is quite possible, however.

The loss of spectral weight is larger for the minority-spin band, thereby enhancing the spin polarization at E_F . The photoemission data suggest that similar enhancements of the spin polarization might occur in magnetotransport and could be used in magnetoelectronic devices. For example, the spin polarization observed in spin tunneling from Ni exceeds the traditional density-of-states model by a factor of 5. The analogy with photoemission suggests that the tunneling matrix element might be responsible.

ACKNOWLEDGMENTS

We would like to acknowledge stimulating discussions with J. C. Campuzano, R. Joynt, A. Chubukov, and J. Allen on many-electron effects and the spectral function. This work was supported by the NSF under Award Nos. DMR-9815416 and DMR-9704196 and DMR-9809423, and by D.O.E. Grant No. DE-FG02-96ER45595. It was conducted at the SRC, which is supported by the NSF under Award No. DMR-9531009.

-
- ¹A series of articles on magnetoelectronics is published in: Phys. Today **48**, 24 (1995).
- ²G. A. Prinz, J. Magn. Magn. Mater. **200**, 57 (1999).
- ³F. J. Himpsel, J. E. Ortega, G. J. Mankey, and R. F. Willis, Adv. Phys. **47**, 511 (1998).
- ⁴R. Meservey and P. M. Tedrow, Phys. Rep. **238**, 173 (1994).
- ⁵J. S. Moodera, J. Nowak, and R. J. M. van de Veerdonk, Phys. Rev. Lett. **80**, 2941 (1998).
- ⁶M. Bode, M. Getzlaff, and R. Wiesendanger, Phys. Rev. Lett. **81**, 4256 (1998).
- ⁷W. Wulfhekel and J. Kirschner, Appl. Phys. Lett. **75**, 1944 (1999).
- ⁸T.-H. Kim, Y.-J. Choi, W.-G. Park, Y. Obukhov, and Y. Kuk, *Proceedings of STM'99*, edited by Y. Kuk, I. W. Lyo, D. Jeon, and S.-I. Park (Seoul, 1999) p. 224.
- ⁹M. B. Stearns, J. Magn. Magn. Mater. **5**, 167 (1977).
- ¹⁰J. C. Slonczewski, Phys. Rev. B **39**, 6995 (1989).
- ¹¹J. Mathon, Phys. Rev. B **56**, 11 810 (1997).
- ¹²J. M. MacLaren, X. D. Zhang, and W. H. Butler, Phys. Rev. B **56**, 11 827 (1997).
- ¹³E. Y. Tsymbal and D. G. Pettifor, J. Phys.: Condens. Matter **9**, L411 (1997).
- ¹⁴D. Y. Petrovykh, K. N. Altmann, H. Höchst, M. Laubscher, S. Maat, G. J. Mankey, and F. J. Himpsel, Appl. Phys. Lett. **73**, 3459 (1998).
- ¹⁵F. J. Himpsel, K. N. Altmann, G. J. Mankey, J. E. Ortega, and D. Y. Petrovykh, J. Magn. Magn. Mater. **200**, 456 (1999).
- ¹⁶F. Manghi, V. Bellini, J. Osterwalder, T. J. Kreuz, P. Aebi, and C. Arcangeli, Phys. Rev. B **59**, R10 409 (1999).
- ¹⁷I. I. Mazin, Phys. Rev. Lett. **83**, 1427 (1999).
- ¹⁸R. J. Soulen, J. M. Byers, M. S. Osofsky, B. Nadgorny, T. Ambrose, S. F. Cheng, P. R. Broussard, C. T. Tanaka, J. Nowak, J. S. Moodera, A. Barry, and J. M. D. Coey, Science **282**, 85 (1998).
- ¹⁹S. K. Upadhyay, A. Palanisami, R. N. Louie, and R. A. Buhrman, Phys. Rev. Lett. **81**, 3247 (1998).
- ²⁰F. J. Himpsel, Adv. Phys. **32**, 1 (1983).
- ²¹C. Guillot, Y. Ballu, J. Paigné, J. Lecante, K. P. Jain, P. Thiry, R. Pinchaux, Y. Péroff, and L. M. Falicov, Phys. Rev. Lett. **39**, 1632 (1977).
- ²²M. Iwan, F. J. Himpsel, and D. E. Eastman, Phys. Rev. Lett. **43**, 1829 (1979).
- ²³F. J. Himpsel, P. Heimann, and D. E. Eastman, J. Appl. Phys. **52**, 1658 (1981).
- ²⁴F. J. Himpsel, J. A. Knapp, and D. E. Eastman, Phys. Rev. B **19**, 2919 (1979).
- ²⁵A. Liebsch, Phys. Rev. Lett. **43**, 1431 (1979); Phys. Rev. B **23**, 5203 (1981).
- ²⁶W. Nolting, W. Borgiel, V. Dose, and Th. Fauster, Phys. Rev. B **40**, 5015 (1989).
- ²⁷L. C. Davis, J. Appl. Phys. **59**, R25 (1986).
- ²⁸M. Springer, F. Aryasetiawan, and K. Karlsson, Phys. Rev. Lett. **80**, 2389 (1998).
- ²⁹H.-J. Freund, W. Eberhardt, D. Heskett, and E. W. Plummer, Phys. Rev. Lett. **50**, 768 (1983).
- ³⁰S. W. Robey, V. E. Henrich, C. Eylem, and B. W. Eichhorn, Phys. Rev. B **52**, 2395 (1995).
- ³¹The sudden approximation is made, which is reasonable at high

photon energies, such as those in this paper. The sum over final states in the *golden rule* expression for photoemission²⁰ is neglected over the narrow E and \mathbf{k} range considered here.

³²G. J. Mankey (unpublished).

³³For the band topology of Ni along the Σ axis compare Ref. 15, Fig. 1. The location of the transitions in \mathbf{k} space is given in Fig. 4 of Ref. 15. In this ‘‘transverse’’ geometry the k^\perp broadening induced by the finite escape depth is eliminated to first order because the broadened k^\perp component lies tangent to the Fermi surface. Synchrotron radiation was used with p -polarized light

incident 60° from the emission direction for the (100) surfaces and 50° for the (110) surfaces, with the sample normal between the photons and electrons. The spectra in Fig. 1 were acquired simultaneously over E, \mathbf{k} using a Scienta electron spectrometer. The sample temperature was 200 K, which sharpened the spectral features near E_F compared to room temperature.

³⁴Typical models for $\Gamma(\omega, \mathbf{k})$ contain terms proportional to ω^2 and T^2 , in addition to a k^2 term. These are incorporated into an effective $\Gamma(\mathbf{k})$, which also takes an experimental broadening into account.